

# Direct mass measurements of neutron-rich zinc and gallium isotopes: an investigation of the formation of the first r-process peak

Andrew Jacobs,<sup>1,2,\*</sup> Stylianos Nikas,<sup>3</sup> John Ash,<sup>1</sup> Behnam Ashrafkhani,<sup>1,4</sup> Ivana Belosovic,<sup>1</sup> Julian Bergmann,<sup>5</sup> Callum Brown,<sup>6</sup> Jaime Cardona,<sup>1,7</sup> Eleanor Dunling,<sup>1</sup> Timo Dickel,<sup>5,8</sup> Gabriella Gelinas,<sup>1,4</sup> Zach Hockenbery,<sup>1,9</sup> Sakshi Kakkar,<sup>1,7</sup> Brian Kootte,<sup>1,7</sup> Ali Mollaebrahimi,<sup>1,5</sup> Eleni Marina Lykiardopoulou,<sup>1,2</sup> Tobias Murböck,<sup>1,5</sup> Stefan Paul,<sup>1</sup> Wolfgang R. Plaß,<sup>5,8</sup> William S. Porter,<sup>1,10</sup> Moritz Pascal Reiter,<sup>1,6</sup> Alex Ridley,<sup>1</sup> Jon Ringuette,<sup>1,11</sup> Christoph Scheidenberger,<sup>5,8,12</sup> Rane Simpson,<sup>1,2</sup> Coulter Walls,<sup>1,7</sup> Yilin Wang,<sup>1,2</sup> Jens Dilling,<sup>13</sup> and Ania Kwiatkowski<sup>1,14</sup>

<sup>1</sup>*TRIUMF, 4004 Westbrook Mall, Vancouver, V6T 1Z1, BC, Canada*

<sup>2</sup>*Department of Physics and Astronomy, University of British Columbia, 6224 Agricultural Rd, Vancouver, V6T 1Z1, BC, Canada*

<sup>3</sup>*University of Jyväskylä, P.O. Box 35, FI-40014 University of Jyväskylä, Finland*

<sup>4</sup>*Department of Physics and Astronomy, University of Calgary, 2500 University Drive NW, Calgary, T2N 1N4, Alberta, Canada*

<sup>5</sup>*II. Physikalisches Institut, Justus-Liebig-Universität Gießen, Gießen, 35392, Hessen, Germany*

<sup>6</sup>*Institute for Particle and Nuclear Physics, University of Edinburgh, Peter Guthrie Tait Road, Edinburgh, EH9 3FD, United Kingdom*

<sup>7</sup>*Department of Physics and Astronomy, University of Manitoba, 30A Sifton Road, Winnipeg, R3T 2N2, Manitoba, Canada*

<sup>8</sup>*GSI Helmholtzzentrum für Schwerionenforschung GmbH, 64291 Darmstadt, Germany*

<sup>9</sup>*Department of Physics, McGill University, 3600 Rue University, Montréal, QC H3A 2T8, Canada*

<sup>10</sup>*Department of Physics and Astronomy, University of Notre Dame, Notre Dame, IN 46556, USA*

<sup>11</sup>*Department of Physics, Colorado School of Mines, Golden, Colorado 80401, USA*

<sup>12</sup>*Helmholtz Research Academy Hesse for FAIR (HFHF),*

*GSI Helmholtz Center for Heavy Ion Research, Campus Gießen, 35392 Gießen, Germany*

<sup>13</sup>*Oak Ridge National Laboratory, 1 Bethel Valley Road, Oak Ridge, 37831, TN, United States*

<sup>14</sup>*Department of Physics and Astronomy, University of Victoria, 3800 Finnerty Road, Victoria, V8P 5C2, BC, Canada*

(Dated: September 22, 2023)

The prediction of isotopic abundances resulting from the rapid neutron capture process (r-process) requires high-precision mass measurements. Mass measurements of  $^{79-83}\text{Zn}$  and  $^{85,86}\text{Ga}$  using TRIUMF's on-line time-of-flight spectrometer. First time measurements are performed for  $^{79m}\text{Zn}$ ,  $^{83}\text{Zn}$ , and  $^{86}\text{Ga}$ . These measurements reduced uncertainties, and are used to calculate isotopic abundances near the first r-process abundance peak using astrophysical conditions present during a binary neutron star (BNS) merger. Good agreement across a range of trajectories is found when comparing to several metal-poor stellar abundances. Particularly, this subset of trajectories produces agreement with the abundance pattern of both the 'r/s-star' HD94028 as well as the 'r-process star' HD222925. These findings point to a high degree of sensitivity to the electron fraction of a BNS merger on the final elemental abundance pattern near the first r-process peak. In particular, we find that small changes in electron fraction produce distinct abundance patterns that match those of metal-poor stars with different classifications, calls the need for an i-process into question.

The formulation of the synthesis of elements heavier than Fe identifies two processes corresponding to neutron captures [1]. They differentiate between an environment with a low neutron density ( $\approx 10^6 - 10^{10} \text{ cm}^{-3}$ ) resulting in a slow capture process (s-process) [2], and an environment with a high neutron density ( $\approx 10^{20} \text{ cm}^{-3}$ ) leading to a rapid capture process (r-process) [3]. Since then, both the s- and r-processes have been separated into 'main' and 'weak' components with different astrophysical sites correlating to each [4–9].

Significant developments have been achieved regarding the r-process following the detection of the Binary Neutron Star (BNS) merger GW170917 [10] and its subsequent kilonova AT2017gfo [11, 12]. From the electromagnetic spectrum, an early blue emission indicates a

moderate r-process environment where isotope production up to  $A \leq 140$  occurred. Furthermore, Sr isotopes specifically have been identified in the spectra [13] proving the production of light elements around the 1<sup>st</sup> abundance peak. The blue emission is followed by a red emission which indicates the production of heavy elements up to lanthanides. Due to the path the r-process takes, nucleosynthesis modeling often requires the use of nuclear models to provide the necessary nuclear inputs where data is lacking. As such, it is imperative to provide experimental data for key nuclei along the r-process path, particularly mass values [14–18]. Conversely, occurring close to the 'valley of beta stability' where almost all needed nuclear data is available, the s-process is comparatively well understood [19].

However, both s- and r-process models fail to describe the isotopic abundances of pre-solar grains [20–23] and elemental abundance patterns found in particular stars (termed ‘r/s-stars’ or ‘i-stars’) [24–26]. Two notable inconsistencies found between solar r-process abundance predictions and r/s-stars are the Ge-As-Se triplet [27, 28] and the enhanced abundances of elements from  $38 \leq Z \leq 48$ . A solution was developed by utilizing a neutron capture process, termed the intermediate neutron capture process (i-process) [29–32]. Despite the i-process successfully reproducing stellar abundances between the 1<sup>st</sup> and 2<sup>nd</sup> r-process abundance peaks, where combinations of s- and r-processes only have previously failed [33], and demonstrating the production of actinides in low metallicity AGB stars [34], its existence and validity remains under discussion [35–37].

In this Letter we report the first direct mass measurements of  $^{83}\text{Zn}$  and  $^{86}\text{Ga}$  as well as an improved mass uncertainty of  $^{85}\text{Ga}$ . We revisit the formation of elements from  $32 \leq Z \leq 48$  with state-of-the-art r-process nucleosynthesis calculations in an astrophysical environment conducive to that of a BNS merger. We show that, when including new experimental values, the blue kilonova can reproduce the previously challenging abundance ratios of both: r-process enhanced stars such as HD222925 [38] and typical r/s-stars which motivate the existence of the i-process such as HD94028 [33].

High precision mass measurements were performed at TRIUMF’s Ion Trap for Atomic and Nuclear science (TITAN) [39] located in the Isotope Separator and ACcelerator (ISAC) [40] facility at TRIUMF in Vancouver, Canada. This facility provides access to short-lived radioactive isotopes involved in these processes. In this Letter, we report the first science results from the novel target developed at TRIUMF-ISAC utilizing a W-neutron converter [41].

A resonant laser ionization [42] was used for Zn, and standard surface ionization was employed for other species [43]. The radioactive ion beam (RIB) was reduced to a single A/q by a magnetic dipole mass separator [44] and delivered to TITAN in order to perform a high precision mass measurement using the MR-TOF-MS.

The TITAN MR-TOF-MS [45, 46] is based on the Gießen-GSI design used at the FRS Ion-Catcher [47–49]. The measurements were performed following an established procedure [46, 50]. In addition, a newly developed technique was used to achieve the needed beam purity. To perform this operation, the potentials of the MR-TOF-MS mirror closer to the injection trap can be lowered, and the ions are dynamically re-captured in the injection trap. This process, called mass selective re-trapping [51, 52], enables the suppression of isobaric contamination by up to four orders of magnitude and has been utilized in several on-line experiments at TITAN [53–56].

To extract the masses of the species of interest, a data

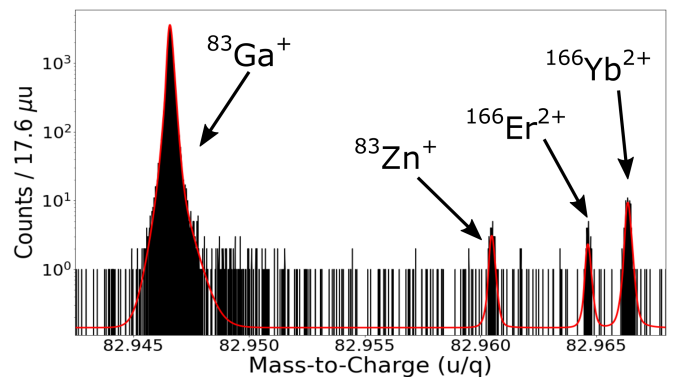


FIG. 1. The spectrum and fit (red) for  $A/q = 83$  at 900 turns after 2.5 hours accumulation.  $^{83}\text{Ga}^+$  has been used as the calibration species.

analysis procedure using the methodologies described in [57, 58] was performed. A resulting spectrum in which the mass of  $^{83}\text{Zn}$  was determined can be seen in figure 1. To maximize the resolving power of the system, a time-resolved calibration (TRC) is done [57]. For the first time, a newly developed ion manipulation technique referred to as ‘post re-trapping beam merging’ was used to ensure that a TRC species was available, regardless of RIB composition. This technique is performed between the isobar separation and mass measurement steps. This allows the merging of the isobarically purified ion ensemble with a controlled amount of an additional stable calibration species. In this particular experiment, post re-trapping beam merging was used to achieve a sufficient resolving power needed to separate  $^{86}\text{Rb}^+$  and  $^{86m}\text{Rb}^+$  via a  $^{85}\text{Rb}^+$  TRC. As such, an isobaric calibration species is provided for  $^{86}\text{Ga}^+$ . This, in turn, made the first high-precision measurement of  $^{86}\text{Ga}^+$  possible. Details on this novel technique are described in [52].

The EMGFIT Python package [59] was then used to fit the peak centroids using a hyper-exponentially modified Gaussian lineshape [60]. From the centroids, a well-measured calibration species is used to extract the final mass of the species of interest. Statistical and systematic uncertainties are determined using the procedures described in [57, 58]. Ultimately, a systematic uncertainty of  $\delta m/m = 1 \cdot 10^{-7}$  has been determined for these measurements resulting in absolute uncertainties of  $\delta m < 20 \text{ keV}/c^2$ .

Table I provides a list of the measured masses for  $^{79-83}\text{Zn}$  and  $^{85,86}\text{Ga}$ . The calibration species as well as the mass ratios are reported to account for any adjustment in the calibrant masses in the future. The mass excess results ( $\text{ME}_{\text{TITAN}}$ ), previous high precision measurements ( $\text{ME}_{\text{AME2020}}$ ) [61], and the difference between the two are reported.

All results are in good agreement with literature values. The uncertainty of  $^{85}\text{Ga}$ , reported by TITAN in [62],

Species	Calibrant	Mass Ratio	ME <sub>TITAN</sub> (keV/c <sup>2</sup> )	ME <sub>AME2020</sub> (keV/c <sup>2</sup> )	Difference (keV/c <sup>2</sup> )
<sup>79</sup> Zn	<sup>79</sup> Ga	1.000136781 (51)	-53430.0 (79)	-53432.3 (22)	2.3 (8.4)
<sup>79m</sup> Zn	<sup>79</sup> Ga	1.00013678 (16)	-52491 (14)	-52330 (150)	161 (151)
<sup>80</sup> Zn	<sup>80</sup> Rb	1.000275561 (48)	-51661 (10)	-51648.6 (26)	-12 (11)
<sup>81</sup> Zn	<sup>81</sup> Ga	1.00015146 (11)	-46209 (12)	-46200 (5)	-9 (13)
<sup>82</sup> Zn	<sup>82</sup> Ga	1.000139116 (91)	-42312 (10)	-42314 (3)	2 (10)
<sup>83</sup> Zn	<sup>83</sup> Ga	1.00016756 (22)	-36311 (18)	###	###
<sup>85</sup> Ga	<sup>85</sup> Rb	1.00053666 (15)	-39720 (14)	-39740 (40)	20 (42)
<sup>86</sup> Ga	<sup>86</sup> Rb	1.00061203 (23)	-33768 (20)	###	###

TABLE I. Ga and Zn mass measurements with their respective calibrants, mass ratios ( $m_{species}/m_{cal}$ ), and mass excess results (ME<sub>TITAN</sub>) compared to the most recent AME2020 mass excess (ME<sub>AME2020</sub>). All species were measured in the singly charged (1+) state. Mass Excesses (ME) and mass ratios are reported as atomic masses. Previously unmeasured species are marked as ###.

has been reduced by a factor  $\approx 3$  and is in agreement with the previous value. Additionally, the excitation energy of <sup>79m</sup>Zn was measured for the first time using direct mass spectrometry techniques, and its uncertainty has been reduced by an order of magnitude. Lastly, first direct measurements of <sup>83</sup>Zn and <sup>86</sup>Ga have been performed.

To interpret the impact of these results, we use the statistical model code TALYS [63] to calculate the corresponding (n,  $\gamma$ ) reaction rates with the new mass values. Two different mass tables were used. The first mass table used experimental nuclear masses from AME2020 and, where experimental data is unavailable, the FRDM2012 mass tables [64] (referred to henceforth as AME+FRDM). The second mass table used the same combination of AME2020 and FRDM2012, but included the new and improved TITAN mass values in place of either AME2020 or FRDM2012 values (referred to as TITAN).

The transmission coefficients for the formation of the compound nucleus are calculated from a spherical neutron-nucleus optical potential using the Koning-Delaroche globally fitted parameters [65]. The Back-Shifted Fermi Gas model is used [66, 67] to describe level densities, and the Kopecky-Uhl generalized Lorentzian [68] is used for the  $\gamma$  strength functions. The reaction rates were calculated for each mass table using the corresponding central mass values to calculate the reaction Q-values. A set of 100 random variations of the masses within the  $1\sigma$  uncertainty band of known masses and the reported error of  $\sigma_{th} = 0.5595$  MeV from FRDM2012 [64] were generated in order to probe the effect of the isotope’s mass uncertainty for each astrophysical trajectory.

The nuclear reaction network code GSI<sub>Net</sub> was used to model the r-process and calculate the elemental abundances [69]. We initialized calculations at Nuclear Statistical Equilibrium (NSE), setting the initial temperature as  $T_0 = 10$  GK. Due to the uncertainties in the astrophysical conditions that could produce nuclei in the first r-process peak region ( $A \approx 82$ ), we simulated nucleosynthesis for a set of parameterized r-process tra-

jectories where we treat initial electron fraction ( $Y_e = N_p/(N_p + N_n)$ ) as a free parameter to investigate. This range is encompassed by expected electron fractions found in BNS mergers.

The expansion time scale was set as  $\tau = 7$  ms, and the initial specific entropy as  $15 k_B$ / baryon. We assume that the density evolution of the ejecta initially follows an exponential expansion and at later times a homologous expansion [70]. We evolve our abundances assuming NSE for  $T \geq 6$  GK, before changing to the full nuclear network calculations.

Previous work at the first r-process peak has shown a remarkable agreement between parts of the solar r-process abundances and predictions from r-process network calculations [62]. However, due to its age, the Sun has likely undergone several enrichment events [71]. As such, metal-poor (i.e. old) stars offer additional insights due to experiencing fewer enrichment events. In this work we explore the abundances of the r-process star HD222925 [38], which has one of the most complete abundance sets for any object beyond the solar system, and the r/s-star HD94028 [33] which has been a key motivator for the existence of the i-process.

Following the calculation of each elemental abundance, the results were normalized for each value of  $Y_e$  to the abundance of Se ( $Z = 34$ ). To allow comparison, this procedure was also applied to the measured abundance patterns of HD94028 [33] and HD222925 [38]. In Figure 2, the resulting abundances for a selection of  $Y_e$ s is shown from  $Z = 32 - 48$  compared to the observed abundance patterns. We find that, by varying  $Y_e$  in a narrow range, the resulting abundance pattern can better match that of either HD94028 or HD222925 ( $Y_e = 0.336$  and  $0.354$  respectively, which is within the range of  $Y_e$  estimated from a blue kilonova [72, 73]). However, a strong odd-even effect from  $Z = 38 - 40$  is not reproduced for any value of  $Y_e$ , and the optimal  $Y_e$  for reproducing the abundance pattern of HD222925 at  $Z = 32 - 34$  drastically underproduces elements of  $Z > 42$ . In the lower half of Figure 2, the residuals between HD94028 and HD222925 and

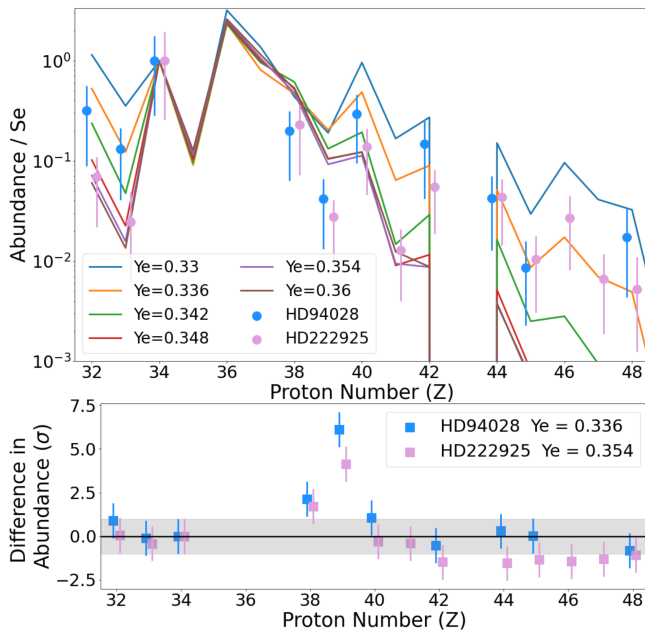


FIG. 2. (Top) Calculated elemental abundances of the 1st r-process for a wide range of  $Y_e$  normalized to Se using AME2020 and new TITAN mass data compared to the abundance patterns of HD94028 (r/s-star), and HD222925 (r-star). (Bottom) The difference in abundances for HD94028 and HD222925 from their optimal  $Y_e$  normalized to the  $1\sigma$  values for the stellar abundances. Thus, within the  $Y_e$  range of a blue kilonova, the abundance patterns for two different stellar classifications can be reproduced.

their optimal  $Y_e$  abundances are shown normalized to the stellar abundance uncertainty ( $\sigma$ ). Very good agreement is found for HD94028 with the exception of Y ( $Z = 39$ ), and HD222925 is somewhat well reproduced with systematic underproduction beyond  $Z = 42$ .

In Figure 3, the abundance results are compared between the two different datasets (AME+FRDM and TITAN). In the upper panel, the differences between AME+FRDM and TITAN are shown for the same  $Y_e$ 's as those seen in Figure 2 (again normalized to Se). In general, the updated TITAN mass values predict an increase in Ge and As ( $Z = 32$  and  $33$ ), a decrease in Br ( $Z = 35$ ), and an increase in all elements beyond by  $\approx 20\%$ . In the lower panel, the change in abundance is shown for  $Y_e = 0.34$  with the respective uncertainties of both datasets. The new mass values reduce the abundance uncertainty by a factor of 2. This increased production beyond  $Z = 35$  due to new mass values can partially explain the anomalous increase in abundance for elements between the 1<sup>st</sup> and 2<sup>nd</sup> r-process peaks for stars such as HD94028.

Certain abundance discrepancies found in stars such as HD94028 have resulted in their classification as r/s-stars [33], namely the high abundances of Ge and As relative to Se as well as increased abundances of ele-

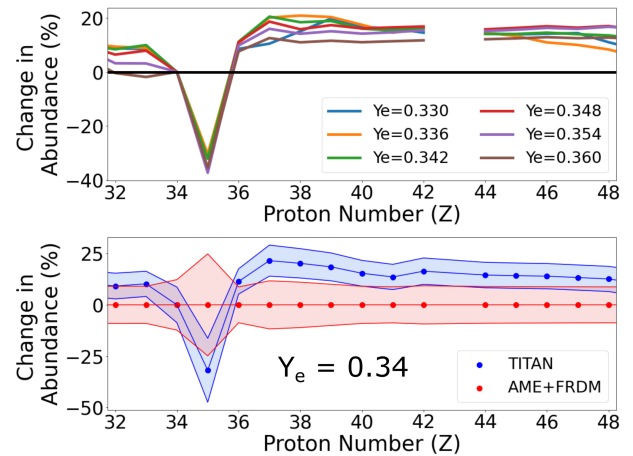


FIG. 3. (Top) The difference in abundance between the TITAN and AME+FRDM datasets for a range of  $Y_e$  matching that seen in figure 2. (Bottom) The percent difference between TITAN and AME+FRDM results for  $Y_e = 0.34$  and their corresponding relative uncertainties to  $1\sigma$ . This systematic increase in production for  $Z \geq 36$  aids in addressing the previously thought underproduction by the r-process for these elements.

ments from  $38 \leq Z \leq 48$ . Hence, we investigate the interplay between these key elemental ratios. Figure 4 compares the logarithmic ratios of Ge/Se, As/Se, and Se/Zr for our r-process calculations using the new TITAN mass results (for trajectories of  $Y_e = 0.33 - 0.36$ ), HD94028, HD222925, and several other metal poor stars with reported abundances of Ge, As, Se, and Zr (from [28, 74]). In both plots, we find that our results, across a narrow range of  $Y_e$ , match the general distribution of these metal-poor stars. Moreover, we find that the optimal  $Y_e$  for the Ge-As-Se triplet matches the optimal  $Y_e$  of the Ge-Se-Zr triplet. With such excellent agreement and high sensitivity to  $Y_e$ , we propose that the variability of  $Y_e$  found in a BNS merger can explain seemingly stark differences in stellar abundance patterns around the 1<sup>st</sup> abundance peak without requiring an entirely separate elemental production mechanism.

In summary, we have performed high precision mass measurements of neutron rich Zn and Ge isotopes including first time measurements of <sup>83</sup>Zn and <sup>86</sup>Ga. These measurements were enabled by the development of the new ISAC proton-to-neutron converter target as well as the MR-TOF-MS beam merging technique. With these new mass values, state-of-the-art r-process network calculations were performed for trajectories conducive to the astrophysical environment of a BNS merger's neutrino drive winds which produce a weak r-process. We find that, by varying the initial electron fraction,  $Y_e$ , we can reproduce the abundance patterns of stars with different classifications (namely r/s-star HD94028 and r-process star HD222925). Furthermore, we find that by varying  $Y_e$ , we reproduce the correlations between key elemental

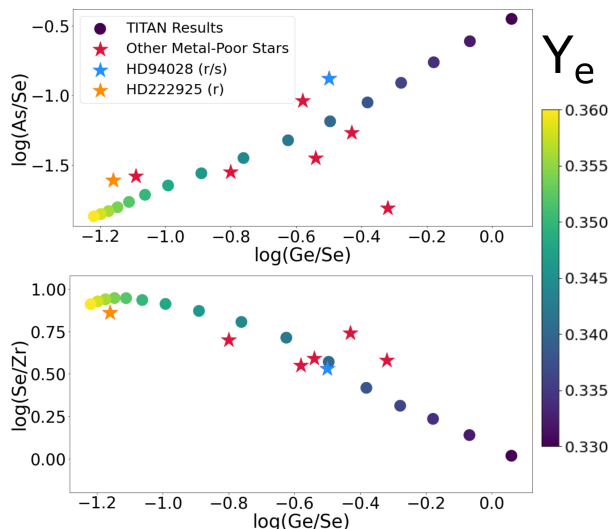


FIG. 4. Comparison of logarithmic ratios of key element pairs between TITAN results (with an additional color scale axis for  $Y_e = 0.33 - 0.36$  in steps of 0.002) and observations of various metal-poor stars. The trend in ratios from observational stellar data matches that of the  $Y_e$  range produced by a blue kilonova.

ratios (Ge/Se, As/Se, and Se/Zr) of several metal-poor stars. Ultimately, these results point to the possibility that, for a given astrophysical site, small differences in  $Y_e$  can explain large observed deviations in abundance patterns near the first r-process peak. As such, this result calls into question the explicit need for an i-process to explain the observed abundances in r/s-stars such as HD94028. To further test these conclusions, additional abundance observations from HD94028 and HD222925 for  $35 \leq Z \leq 37$  and from  $32 \leq Z \leq 48$  of metal-poor stars (such as those in Reticulum II [75]) would prove particularly useful.

We would like to thank the Targets and Ion Source group at TRIUMF. Particularly, thank J. Lassen for the Zn laser development as well as A. Gottberg and L. Egoriti for the proton-to-neutron converter target development. Additionally, we would like to thank N. Vassh for fruitful discussion pertaining to our results. This work was supported by the Natural Sciences and Engineering Research Council (NSERC) of Canada under Grants No. SAPIN-2018-00027, No. RGPAS-2018-522453, and No. SAPPJ-2018-00028, the National Research Council (NRC) of Canada through TRIUMF, the Canada-UK Foundation, German institutions DFG (grants FR 601/3-1, SCHE 1969/2-1 and SFB 1245 and through PRISMA Cluster of Excellence), BMBF (grants 05P19RGFN1 and 05P21RGFN1), and by the JLU and GSI under the JLU-GSI strategic Helmholtz partnership agreement.

\* Corresponding author: ajacobs@triumf.ca

- [1] E. M. Burbidge, G. R. Burbidge, W. A. Fowler, and F. Hoyle, Synthesis of the elements in stars, *Rev. Mod. Phys.* **29**, 547 (1957).
- [2] F. Käppeler, R. Gallino, S. Bisterzo, and W. Aoki, The s process: Nuclear physics, stellar models, and observations, *Rev. Mod. Phys.* **83**, 157 (2011).
- [3] C. J. Horowitz, A. Arcones, B. Côté, I. Dillmann, W. Nazarewicz, I. U. Roederer, H. Schatz, A. Aprahamian, D. Atanasov, A. Bauswein, T. C. Beers, J. Bliss, M. Brodeur, J. A. Clark, A. Frebel, F. Foucart, C. J. Hansen, O. Just, A. Kankainen, G. C. McLaughlin, J. M. Kelly, S. N. Liddick, D. M. Lee, J. Lippuner, D. Martin, J. Mendoza-Temis, B. D. Metzger, M. R. Mumpower, G. Perdikkakis, J. Pereira, B. W. O'Shea, R. Reifarh, A. M. Rogers, D. M. Siegel, A. Spyrou, R. Surman, X. Tang, T. Uesaka, and M. Wang, r-process nucleosynthesis: connecting rare-isotope beam facilities with the cosmos, *Journal of Physics G: Nuclear and Particle Physics* **46**, 083001 (2019).
- [4] N. Prantzos, M. Hashimoto, and K. Nomoto, The s-process in massive stars-yields as a function of stellar mass and metallicity, *Astron. Astrophys.* **234**, 211 (1990).
- [5] M. Busso, R. Gallino, and G. Wasserburg, Nucleosynthesis in asymptotic giant branch stars: Relevance for galactic enrichment and solar system formation, *Annual Review of Astronomy and Astrophysics* **37**, 239 (1999).
- [6] C. Winteler, R. Kaeppeli, A. Perego, A. Arcones, N. Vasset, N. Nishimura, M. Liebendoerfer, and F.-K. Thielemann, Magnetorotationally driven supernovae as the origin of early galaxy r-process elements?, *Astrophys. J. Lett.* **750**, L22 (2012).
- [7] S. Wanajo, The r-process in proto-neutron-star wind revisited, *Astrophys. J. Lett.* **770**, L22 (2013).
- [8] S. Wanajo, B. Müller, H.-T. Janka, and A. Heger, Nucleosynthesis in the innermost ejecta of neutrino-driven supernova explosions in two dimensions, *Astrophys. J.* **852**, 40 (2018).
- [9] D. M. Siegel, J. Barnes, and B. D. Metzger, Collapsars as a major source of r-process elements, *Nature* **569**, 241 (2019).
- [10] B. P. Abbott, R. Abbott, T. Abbott, F. Acernese, K. Ackley, C. Adams, T. Adams, P. Addesso, R. Adhikari, V. B. Adya, *et al.*, GW170817: observation of gravitational waves from a binary neutron star inspiral, *Phys. Rev. Lett.* **119**, 161101 (2017).
- [11] B. P. Abbott, R. Abbott, T. Abbott, F. Acernese, K. Ackley, C. Adams, T. Adams, P. Addesso, R. Adhikari, V. Adya, *et al.*, Gravitational waves and gamma-rays from a binary neutron star merger: GW170817 and GRB 170817A, *Astrophys. J. Lett.* **848**, L13 (2017).
- [12] D. Kasen, B. Metzger, J. Barnes, E. Quataert, and E. Ramirez-Ruiz, Origin of the heavy elements in binary neutron-star mergers from a gravitational-wave event, *Nature* **551**, 80 (2017).
- [13] D. Watson, C. J. Hansen, J. Selsing, A. Koch, D. B. Malesani, A. C. Andersen, J. P. Fynbo, A. Arcones, A. Bauswein, S. Covino, *et al.*, Identification of strontium in the merger of two neutron stars, *Nature* **574**, 497 (2019).

- [14] S. Brett, I. Bentley, N. Paul, R. Surman, and A. Aprahamian, Sensitivity of the r-process to nuclear masses, *The European Physical Journal A* **48**, 1 (2012).
- [15] A. Aprahamian, I. Bentley, M. Mumpower, and R. Surman, Sensitivity studies for the main r process: nuclear masses, *AIP Advances* **4**, 041101 (2014), <https://doi.org/10.1063/1.4867193>.
- [16] M. R. Mumpower, R. Surman, D.-L. Fang, M. Beard, P. Möller, T. Kawano, and A. Aprahamian, Impact of individual nuclear masses on r-process abundances, *Phys. Rev. C* **92**, 035807 (2015).
- [17] M. Mumpower, R. Surman, D. L. Fang, M. Beard, and A. Aprahamian, The impact of uncertain nuclear masses near closed shells on the r-process abundance pattern, *J. Phys. G Nucl. Part. Phys.* **42**, 034027 (2015).
- [18] X. F. Jiang, X. H. Wu, and P. W. Zhao, Sensitivity study of r-process abundances to nuclear masses, *Astrophys. J.* **915**, 29 (2021).
- [19] R. Reifarh, C. Lederer, and F. Käppeler, Neutron reactions in astrophysics, *Journal of Physics G: Nuclear and Particle Physics* **41**, 053101 (2014).
- [20] W. Fujiya, P. Hoppe, E. Zinner, M. Pignatari, and F. Herwig, Evidence for radiogenic sulfur-32 in type AB presolar silicon carbide grains?, *Astrophys. J. Lett.* **776**, L29 (2013).
- [21] M. Jadhav, M. Pignatari, F. Herwig, E. Zinner, R. Gallino, and G. R. Huss, Relics of ancient post-AGB stars in a primitive meteorite, *Astrophys. J. Lett.* **777**, L27 (2013).
- [22] N. Liu, M. R. Savina, A. M. Davis, R. Gallino, O. Straniero, F. Gyngard, M. J. Pellin, D. G. Willingham, N. Dauphas, M. Pignatari, *et al.*, Barium isotopic composition of mainstream silicon carbides from murchison: Constraints for s-process nucleosynthesis in asymptotic giant branch stars, *Astrophys. J.* **786**, 66 (2014).
- [23] N. Liu, T. Stephan, S. Cristallo, R. Gallino, P. Boehnke, L. R. Nittler, C. M. Alexander, A. M. Davis, R. Trappitsch, M. J. Pellin, *et al.*, Presolar silicon carbide grains of types Y and Z: Their molybdenum isotopic compositions and stellar origins, *Astrophys. J.* **881**, 28 (2019).
- [24] K. Jonsell, P. Barklem, B. Gustafsson, N. Christlieb, V. Hill, T. C. Beers, and J. Holmberg, The Hamburg/ESO R-process enhanced star survey (HERES)-III. HE 0338-3945 and the formation of the r+s stars, *Astron. Astrophys.* **451**, 651 (2006).
- [25] M. Lugaro, A. I. Karakas, R. J. Stancliffe, and C. Rijs, The s-process in asymptotic giant branch stars of low metallicity and the composition of carbon-enhanced metal-poor stars, *Astrophys. J.* **747**, 2 (2012).
- [26] M. Hampel, R. J. Stancliffe, M. Lugaro, and B. S. Meyer, The intermediate neutron-capture process and carbon-enhanced metal-poor stars, *Astrophys. J.* **831**, 171 (2016).
- [27] I. U. Roederer, H. Schatz, J. E. Lawler, T. C. Beers, J. J. Cowan, A. Frebel, I. I. Ivans, C. Sneden, and J. S. Sobeck, New detections of arsenic, selenium, and other heavy elements in two metal-poor stars, *Astrophys. J.* **791**, 32 (2014).
- [28] R. Peterson, B. Barbuy, and M. Spite, Trans-iron Ge, As, Se, and heavier elements in the dwarf metal-poor stars HD 19445, HD 84937, HD 94028, HD 140283, and HD 160617, *Astron. Astrophys.* **638**, A64 (2020).
- [29] J. J. Cowan and W. K. Rose, Production of  $^{14}\text{C}$  and neutrons in red giants., *Astrophys. J.* **212**, 149 (1977).
- [30] T. Suda and M. Y. Fujimoto, Evolution of low-and intermediate-mass stars with  $[\text{Fe}/\text{H}] \leq -2.5$ , *Monthly Notices of the Royal Astronomical Society* **405**, 177 (2010).
- [31] M. Cruz, A. Serenelli, and A. Weiss, S-process in extremely metal-poor, low-mass stars, *Astron. Astrophys.* **559**, A4 (2013).
- [32] P. A. Denissenkov, F. Herwig, P. Woodward, R. Andrassy, M. Pignatari, and S. Jones, The i-process yields of rapidly accreting white dwarfs from multicycle he-shell flash stellar evolution models with mixing parametrizations from 3d hydrodynamics simulations, *Monthly Notices of the Royal Astronomical Society* **488**, 4258 (2019).
- [33] I. U. Roederer, M. Mateo, J. I. Bailey III, Y. Song, E. F. Bell, J. D. Crane, S. Loebman, D. L. Nidever, E. W. Olszewski, S. A. Shectman, *et al.*, Detailed chemical abundances in the r-process-rich ultra-faint dwarf galaxy reticulum 2, *Astron. J.* **151**, 82 (2016).
- [34] A. Choplin, S. Goriely, and L. Siess, Synthesis of thorium and uranium in asymptotic giant branch stars, *Astron. Astrophys.* **667**, L13 (2022).
- [35] A. Choplin, L. Siess, and S. Goriely, The intermediate neutron capture process-i. development of the i-process in low-metallicity low-mass agb stars, *Astron. Astrophys.* **648**, A119 (2021).
- [36] H. Schatz, Trends in nuclear astrophysics, *J. Phys. G Nuc. Part. Phys.* **43**, 064001 (2016).
- [37] W. Han, L. Zhang, G. Yang, P. Niu, and B. Zhang, Study of the abundance features of the metal-poor star HD 94028, *Astrophys. J.* **856**, 58 (2018).
- [38] I. U. Roederer, J. E. Lawler, E. A. D. Hartog, V. M. Placco, R. Surman, T. C. Beers, R. Ezzeddine, A. Frebel, T. T. Hansen, K. Hattori, E. M. Holmbeck, and C. M. Sakari, The r-process alliance: A nearly complete r-process abundance template derived from ultraviolet spectroscopy of the r-process-enhanced metal-poor star hd 222925\*, *Astrophys. J. Supplement Series* **260**, 27 (2022).
- [39] J. Dilling, P. Bricault, M. Smith, and H. J. Kluge, The proposed TITAN facility at ISAC for very precise mass measurements on highly charged short-lived isotopes, *Nuclear Instruments and Methods in Physics Research Section B: Beam Interactions with Materials and Atoms* **204**, 492 (2003).
- [40] G. C. Ball, L. Buchmann, B. Davids, R. Kanungo, C. Ruiz, and C. E. Svensson, Physics with reaccelerated radioactive beams at TRIUMF-ISAC, *J. Phys. G Nuc. Part. Phys.* **38**, 10.1088/0954-3899/38/2/024003 (2011).
- [41] L. Egoriti, R. Augusto, P. Bricault, T. D. Goodacre, M. Delonca, M. Dierckx, D. Hougbo, L. Popescu, J. Ramos, S. Rothe, T. Stora, and A. Gottberg, Development of a proton-to-neutron converter for radioisotope production at ISAC-TRIUMF, *Journal of Physics: Conference Series* **1067**, 082022 (2018).
- [42] J. Lassen, R. Li, S. Raeder, X. Zhao, T. Dekker, H. Heggen, P. Kunz, C. D. P. Levy, M. Mostamand, A. Teigelhöfer, and F. Ames, Current developments with TRIUMF's titanium-sapphire laser based resonance ionization laser ion source, *Hyperfine Interact.* **238**, 33 (2017).
- [43] M. Dombisky, D. Bishop, P. Bricault, D. Dale, A. Hurst, K. Jayamanna, R. Keitel, M. Olivo, P. Schmor, and G. Stanford, Commissioning and initial operation of a radioactive beam ion source at isac, *Review of Scientific Instruments* **71**, 978 (2000),

<https://doi.org/10.1063/1.1150364>.

- [44] P. Bricault, R. Baartman, M. Dombisky, A. Hurst, C. Mark, G. Stanford, and P. Schmor, TRIUMF-ISAC target station and mass separator commissioning, *Nuclear Physics A* **701**, 49 (2002).
- [45] C. Jesch, T. Dickel, W. R. Plaß, D. Short, S. A. San Andrés, J. Dilling, H. Geissel, F. Greiner, J. Lang, K. G. Leach, W. Lippert, C. Scheidenberger, and M. I. Yavor, The MR-TOF-MS isobar separator for the TITAN facility at TRIUMF, *Hyperfine Interact.* **235**, 97 (2015).
- [46] M. Reiter, S. A. S. Andrés, J. Bergmann, T. Dickel, J. Dilling, A. Jacobs, A. Kwiatkowski, W. Plaß, C. Scheidenberger, D. Short, C. Will, C. Babcock, E. Dunling, A. Finlay, C. Hornung, C. Jesch, R. Klawitter, B. Kootte, D. Lascar, E. Leistenschneider, T. Murböck, S. Paul, and M. Yavor, Commissioning and performance of titan's multiple-reflection time-of-flight mass-spectrometer and isobar separator, *Nucl. Instruments Methods Phys. Res. Sect. A Accel.Spectrometers, Detect. Assoc. Equip.* **1018**, 165823 (2021).
- [47] W. R. Plaß, T. Dickel, and C. Scheidenberger, Multiple-reflection time-of-flight mass spectrometry, *Int. J. Mass Spectrom.* **349-350**, 134 (2013), 100 years of Mass Spectrometry.
- [48] T. Dickel, W. Plaß, A. Becker, U. Czok, H. Geissel, E. Haettner, C. Jesch, W. Kinsel, M. Petrick, C. Scheidenberger, A. Simon, and M. Yavor, A high-performance multiple-reflection time-of-flight mass spectrometer and isobar separator for the research with exotic nuclei, *Nucl. Instruments Methods Phys. Res. Sect. A Accel.Spectrometers, Detect. Assoc. Equip.* **777**, 172 (2015).
- [49] T. Dickel, M. I. Yavor, J. Lang, W. R. Plaß, W. Lippert, H. Geissel, and C. Scheidenberger, Dynamical time focus shift in multiple-reflection time-of-flight mass spectrometers, *Int. J. Mass Spectrom.* **412**, 1 (2017).
- [50] E. Leistenschneider, M. Reiter, S. A. San Andrés, B. Kootte, J. Holt, P. Navrátil, C. Babcock, C. Barberi, B. Barquest, J. Bergmann, *et al.*, Dawning of the  $N = 32$  shell closure seen through precision mass measurements of neutron-rich titanium isotopes, *Phys. Rev. Lett.* **120**, 062503 (2018).
- [51] T. Dickel, W. R. Plaß, W. Lippert, J. Lang, M. I. Yavor, H. Geissel, and C. Scheidenberger, Isobar separation in a multiple-reflection time-of-flight mass spectrometer by mass-selective re-trapping, *Journal of The American Society for Mass Spectrometry* **28**, 1079 (2017).
- [52] A. Jacobs, *Nucl. Instruments Methods Phys. Res. Sect. A Accel.Spectrometers, Detect. Assoc. Equip.* (2023, in prepartaion).
- [53] S. Beck, B. Kootte, I. Dedes, T. Dickel, A. A. Kwiatkowski, E. M. Lykiardopoulou, W. R. Plaß, M. P. Reiter, C. Andreoiu, J. Bergmann, T. Brunner, D. Curien, J. Dilling, J. Dudek, E. Dunling, J. Flowerdew, A. Gaamouci, L. Graham, G. Gwinner, A. Jacobs, R. Klawitter, Y. Lan, E. Leistenschneider, N. Minkov, V. Monier, I. Mukul, S. F. Paul, C. Scheidenberger, R. I. Thompson, J. L. Tracy, M. Vansteenkiste, H.-L. Wang, M. E. Wieser, C. Will, and J. Yang, Mass measurements of neutron-deficient yb isotopes and nuclear structure at the extreme proton-rich side of the  $N = 82$  shell, *Phys. Rev. Lett.* **127**, 112501 (2021).
- [54] I. Mukul, C. Andreoiu, J. Bergmann, M. Brodeur, T. Brunner, K. A. Dietrich, T. Dickel, I. Dillmann, E. Dunling, D. Fusco, G. Gwinner, C. Izzo, A. Jacobs, B. Kootte, Y. Lan, E. Leistenschneider, E. M. Lykiardopoulou, S. F. Paul, M. P. Reiter, J. L. Tracy, J. Dilling, and A. A. Kwiatkowski, Examining the nuclear mass surface of rb and sr isotopes in the  $a \approx 104$  region via precision mass measurements, *Phys. Rev. C* **103**, 044320 (2021).
- [55] C. Izzo, J. Bergmann, K. A. Dietrich, E. Dunling, D. Fusco, A. Jacobs, B. Kootte, G. Kripkó-Koncz, Y. Lan, E. Leistenschneider, E. M. Lykiardopoulou, I. Mukul, S. F. Paul, M. P. Reiter, J. L. Tracy, C. Andreoiu, T. Brunner, T. Dickel, J. Dilling, I. Dillmann, G. Gwinner, D. Lascar, K. G. Leach, W. R. Plaß, C. Scheidenberger, M. E. Wieser, and A. A. Kwiatkowski, Mass measurements of neutron-rich indium isotopes for  $r$ -process studies, *Phys. Rev. C* **103**, 025811 (2021).
- [56] W. S. Porter, B. Ashrafkhani, J. Bergmann, C. Brown, T. Brunner, J. D. Cardona, D. Curien, I. Dedes, T. Dickel, J. Dudek, E. Dunling, G. Gwinner, Z. Hockenbery, J. D. Holt, C. Hornung, C. Izzo, A. Jacobs, A. Javaji, B. Kootte, G. Kripkó-Koncz, E. M. Lykiardopoulou, T. Miyagi, I. Mukul, T. Murböck, W. R. Plaß, M. P. Reiter, J. Ringuette, C. Scheidenberger, R. Silwal, C. Walls, H. L. Wang, Y. Wang, J. Yang, J. Dilling, and A. A. Kwiatkowski, Mapping the  $N = 40$  island of inversion: Precision mass measurements of neutron-rich fe isotopes, *Phys. Rev. C* **105**, L041301 (2022).
- [57] S. Ayet San Andrés, C. Hornung, J. Ebert, W. R. Plaß, T. Dickel, H. Geissel, C. Scheidenberger, J. Bergmann, F. Greiner, E. Haettner, C. Jesch, W. Lippert, I. Mardor, I. Miskun, Z. Patyk, S. Pietri, A. Pihktelev, S. Purushothaman, M. P. Reiter, A. K. Rink, H. Weick, M. I. Yavor, S. Bagchi, V. Charviakova, P. Constantin, M. Diwisch, A. Finlay, S. Kaur, R. Knöbel, J. Lang, B. Mei, I. D. Moore, J. H. Otto, I. Pohjalainen, A. Prochazka, C. Rappold, M. Takechi, Y. K. Tanaka, J. S. Winfield, and X. Xu, High-resolution, accurate multiple-reflection time-of-flight mass spectrometry for short-lived, exotic nuclei of a few events in their ground and low-lying isomeric states, *Phys. Rev. C* **99**, 10.1103/PhysRevC.99.064313 (2019).
- [58] S. F. Paul, J. Bergmann, J. D. Cardona, K. A. Dietrich, E. Dunling, Z. Hockenbery, C. Hornung, C. Izzo, A. Jacobs, A. Javaji, B. Kootte, Y. Lan, E. Leistenschneider, E. M. Lykiardopoulou, I. Mukul, T. Murböck, W. S. Porter, R. Silwal, M. B. Smith, J. Ringuette, T. Brunner, T. Dickel, I. Dillmann, G. Gwinner, M. MacCormick, M. P. Reiter, H. Schatz, N. A. Smirnova, J. Dilling, and A. A. Kwiatkowski, Mass measurements of  $^{60-63}\text{Ga}$  reduce x-ray burst model uncertainties and extend the evaluated  $T = 1$  isobaric multiplet mass equation, *Phys. Rev. C* **104**, 065803 (2021).
- [59] S. F. Paul, emgfit - Fitting of time-of-flight mass spectra with hyper-EMG models (2020).
- [60] S. Purushothaman, S. Ayet San Andrés, J. Bergmann, T. Dickel, J. Ebert, H. Geissel, C. Hornung, W. Plaß, C. Rappold, C. Scheidenberger, Y. Tanaka, and M. Yavor, Hyper-EMG: A new probability distribution function composed of exponentially modified gaussian distributions to analyze asymmetric peak shapes in high-resolution time-of-flight mass spectrometry, *Int. J. Mass Spectrom.* **421**, 245 (2017).
- [61] M. Wang, W. J. Huang, F. G. Kondev, G. Audi, and S. Naimi, The AME 2020 atomic mass evaluation (II).

- Tables, graphs and references, Chinese Physics C **45**, 10.1088/1674-1137/abddaf (2021).
- [62] M. Reiter, S. A. San Andrés, S. Nikas, J. Lippuner, C. Andreoiu, C. Babcock, B. Barquest, J. Bollig, T. Brunner, T. Dickel, *et al.*, Mass measurements of neutron-rich gallium isotopes refine production of nuclei of the first r-process abundance peak in neutron-star merger calculations, Phys. Rev. C **101**, 025803 (2020).
- [63] A. J. Koning, S. Hilaire, and M. C. Duijvestijn, Talys-1.0, Proceedings of the International Conference on Nuclear Data for Science and Technology, (2008).
- [64] P. Möller, A. Sierk, T. Ichikawa, and H. Sagawa, Nuclear ground-state masses and deformations: FRDM(2012), Atomic Data and Nuclear Data Tables **109-110**, 1 (2016).
- [65] A. Koning and J. Delaroche, Local and global nucleon optical models from 1 keV to 200 MeV, Nuclear Physics A **713**, 231–310 (2003).
- [66] W. Dilg, W. Schantl, H. Vonach, and M. Uhl, Level density parameters for the back-shifted fermi gas model in the mass range  $40 < A < 250$ , Nuclear Physics A **217**, 269–298 (1973).
- [67] A. Gilbert and A. G. W. Cameron, A composite nuclear-level density formula with shell corrections, Canadian Journal of Physics **43**, 1446–1496 (1965), <http://dx.doi.org/10.1139/p65-139>.
- [68] J. Kopecky and M. Uhl, Test of gamma-ray strength functions in nuclear reaction model calculations, Phys. Rev. C **41**, 1941 (1990).
- [69] J. d. J. Mendoza-Temis, M.-R. Wu, K. Langanke, G. Martínez-Pinedo, A. Bauswein, and H.-T. Janka, Nuclear robustness of the r process in neutron-star mergers, Phys. Rev. C **92**, 055805 (2015).
- [70] J. Lippuner and L. F. Roberts, r-process lanthanide production and heating rates in kilonovae, Astrophys. J. **815**, 82 (2015).
- [71] S. Goriely, Uncertainties in the solar system r-abundance distribution, Astron. Astrophys. **342**, 881 (1999).
- [72] S. Wanajo, Physical conditions for the r-process. I. radioactive energy sources of kilonovae, Astrophys. J. **868**, 65 (2018).
- [73] M.-R. Wu, J. Barnes, G. Martínez-Pinedo, and B. D. Metzger, Fingerprints of heavy-element nucleosynthesis in the late-time lightcurves of kilonovae, Phys. Rev. Lett. **122**, 062701 (2019).
- [74] I. U. Roederer, C. M. Sakari, V. M. Placco, T. C. Beers, R. Ezzeddine, A. Frebel, and T. T. Hansen, The r-process alliance: a comprehensive abundance analysis of HD 222925, a metal-poor star with an extreme r-process enhancement of  $[\text{Eu}/\text{H}] = -0.14$ , Astrophys. J. **865**, 129 (2018).
- [75] A. P. Ji, A. Frebel, A. Chiti, and J. D. Simon, R-process enrichment from a single event in an ancient dwarf galaxy, Nature **531**, 610 (2016).